



HAL
open science

High-Performance Rare-Earth-Free Fluorophores: toward White LEDs

Anthony Barros, Nicolas Ledos, Rodolphe Valleix, Jérémy Cathalan,
Geneviève Chadeyron, Pierre-Antoine Bouit, Muriel Hissler, Damien Boyer

► **To cite this version:**

Anthony Barros, Nicolas Ledos, Rodolphe Valleix, Jérémy Cathalan, Geneviève Chadeyron, et al.. High-Performance Rare-Earth-Free Fluorophores: toward White LEDs. ACS Applied Optical Materials, 2024, 2 (5), pp.834-841. 10.1021/acsaom.4c00102 . hal-04576141

HAL Id: hal-04576141

<https://hal.science/hal-04576141v1>

Submitted on 15 May 2024

HAL is a multi-disciplinary open access archive for the deposit and dissemination of scientific research documents, whether they are published or not. The documents may come from teaching and research institutions in France or abroad, or from public or private research centers.

L'archive ouverte pluridisciplinaire **HAL**, est destinée au dépôt et à la diffusion de documents scientifiques de niveau recherche, publiés ou non, émanant des établissements d'enseignement et de recherche français ou étrangers, des laboratoires publics ou privés.



Distributed under a Creative Commons Attribution 4.0 International License

1
2
3
4
5
6
7
8
9
10
11
12
13
14
15
16
17
18
19
20
21
22
23
24
25
26
27
28
29
30
31
32
33
34
35
36
37
38
39
40
41
42
43
44
45
46
47
48
49
50
51
52
53
54
55
56
57
58
59
60

High-performance rare-earth-free fluorophores: toward white LEDs

Anthony Barros^a, Nicolas Ledos^b, Rodolphe Valleix^a, Jérémy Cathalan^a, Geneviève Chadeyron^a,

Pierre-Antoine Bouit^b, Muriel Hissler^b, Damien Boyer^{a}*

a. Université Clermont Auvergne, Clermont Auvergne INP, CNRS, ICCF, Clermont-Ferrand, 63000, France.

b. Université de Rennes, CNRS, ISCR - UMR 6226, Rennes, 35000, France.

Keywords: organic fluorophores, photoluminescence, luminescent composites, WLEDs, silicone

ABSTRACT

A series of down-converting organic fluorophores were synthesized in order to cover the full range of the visible spectrum, two π -extended phospholes with blue (B) and red (R) emissions and two difluoroboron β -diketonates with green (G) and yellow (Y) emissions. Their excellent optical

*Corresponding author : damien.boyer@sigma-clermont.fr

1
2
3 performances were evidenced by recording their emission spectra and measuring their
4
5
6 photoluminescent absolute quantum yields in both liquid and solid states. Subsequently, these
7
8
9 fluorophores were incorporated into silicone at 10 wt.% to prepare luminescent composite films.
10
11
12 Their photoluminescent properties were analyzed at room temperature and their CIE chromaticity
13
14
15 coordinates were determined. By strategically combining these films emitting different visible
16
17
18 lights (B, G, Y, R) with commercial blue or violet LED chips, we were able to produce white light
19
20
21 exhibiting a high color rendering index (90) and color correlated temperature close to 4500 K.
22
23
24 Finally, to assess the durability of these composite films and to demonstrate the potential of these
25
26
27 rare-earth-free fluorophores as down-converters phosphors for LED based devices, the stability of
28
29
30 their optical performances was investigated upon thermal and photonic stresses.
31
32
33
34
35
36
37
38

39 1. INTRODUCTION

40
41
42 The emergence of white light-emitting diodes (WLEDs) has resulted in a tremendous
43
44
45 technological shift of lighting and display applications because of their high efficiency, long
46
47
48 lifetime and environmental friendliness compared to fluorescent lamps or incandescent bulbs.
49
50
51 Currently, most WLEDs consist of a blue-emitting InGaN light-emitting diode (LED) chip coated
52
53
54 by a down-converter (DC) phosphor, $Y_3Al_5O_{12}:Ce^{3+}$ (YAG:Ce), which converts a part of the blue
55
56
57
58
59
60

1
2
3 light into yellow light. White light is then produced by the combination of the LED chip and
4
5
6 phosphor emissions ^{1, 2}. Even though YAG:Ce exhibits several advantages like a high quantum
7
8
9 efficiency (QE), broad yellow emission spectrum and a high stability upon thermal or photonic
10
11
12 stresses, the use of this single phosphor presents some drawbacks. Indeed, the obtained white light
13
14
15 is characterized as cold (or cool) white light with a colour correlated temperature (CCT) higher
16
17
18 than 4500 K and a poor colour rendering index (CRI) lower than 80 which does not fulfil the
19
20
21 specifications for most lighting and display applications. Thus, to reach a higher CRI and a warmer
22
23
24 white light, a red-emitting phosphor is commonly added to YAG:Ce ³. A few DC phosphors are
25
26
27 able to convert blue emission of LED chip into red light like sulphide phosphors (SrS:Eu²⁺ or
28
29
30 CaS:Eu²⁺), nitride phosphors (CaAlSiN₃:Eu²⁺, Sr₂Si₅N₈:Eu²⁺ or Ba₂Si₅N₈:Eu²⁺) or fluoride
31
32
33 phosphors (K₂SiF₆:Mn⁴⁺ or KSF: Mn⁴⁺). But the development of a red-emitting phosphor with
34
35
36 high quantum efficiency and stability upon an excitation wavelength range which does not overlap
37
38
39 the YAG:Ce emission is still a major challenge.
40
41
42
43
44
45
46

47 As can be seen in their chemical formula, most DC phosphors for LED applications contain
48
49
50 lanthanide ions and hence have full dependence on rare-earth elements (REEs) that are potentially
51
52
53 facing a serious supply shortage, and their lack of recyclability is destructive to the environment
54
55
56
57
58
59
60

1
2
3
4⁴⁻⁷. Today, about 20% of global REEs are used in clean energy technologies. Among them,
5
6
7 europium, terbium, and yttrium are essential ingredients of phosphors used in general lighting.

8
9
10 Since the demand for REEs will continue to increase dramatically for various technologies, their
11
12
13 prices have been rising constantly, making the cost issue even more crucial.

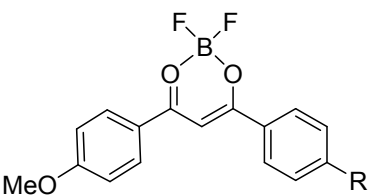
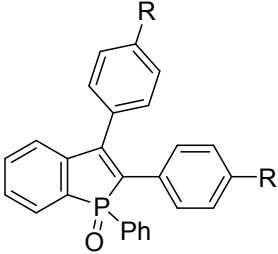
14
15
16
17 Thus, the development of rare-earth-free phosphors is highly important. In this context, the use
18
19
20 of organic fluorophores appears as an appealing strategy. Hence, thanks to the power of organic
21
22
23 synthesis, there exists a wide range of DC fluorophores with tuneable emission wavelengths, high
24
25
26 photoluminescence quantum yields and satisfying chemical/thermal stability. Based on their
27
28
29 successful insertion into various optoelectronic devices such as Organic Light-Emitting Diodes
30
31
32 (OLEDs) or Lasers, we decided to focus on π -extended phospholes and difluoroboron β -
33
34 diketonates for this study (**Table 1**)⁸⁻¹⁰.

35
36
37
38
39
40 Regarding difluoroboron β -diketonate complexes, they display an easy molecular engineering,
41
42
43 excellent solid-state luminescent as well as satisfying stability illustrated by their successful
44
45
46 insertion OLEDs, solar cells or organic lasers¹¹⁻¹³. For these reasons, 1-2 (**Table 1**) were therefore
47
48
49 chosen to be combined with commercial LEDs.
50
51
52
53
54
55
56
57
58
59
60

Besides, the luminescence of π -extended phospholes has been widely exploited in the context of sensing, bioprobes and OLEDs ¹⁴⁻¹⁷.

Their intense luminescence, combined with an easy molecular engineering that allows fine-tuning color and an excellent thermal, chemical and photochemical stability make that π -extended phospholes such 3-4 (**Table 1**) are compounds of choice for being used in WLEDs as rare-earth-free phosphors ¹⁸.

Table 1. Structure and label of the different fluorophores

Structures of fluorophores	R	Name in DCM solution	Name of the powders
	^t Bu	1	P ₁
	H	2	P ₂
	NPh(OMe) ₂	3	P ₃
	H	4	P ₄

1
2
3
4 In this study, four rare-earth-free fluorophores were examined in solution, in solid state, and in
5
6
7 a composite mixture. The optical characteristics of these materials were investigated using UV
8
9
10 spectroscopy, PLQY_{abs} (Absolute Photoluminescence Quantum Yield), emission spectra, and CIE
11
12
13 chromaticity coordinates were also recorded. Luminescent composite films prepared from powders
14
15
16 of these different fluorophores dispersed in silicone were combined with commercial blue and UV
17
18
19 chips to produce white light with tunable color temperature. Finally, the stability under thermal
20
21
22 and photonic stresses of these fluorophores in both powder and composite film forms was
23
24
25
26
27 investigated.
28
29
30
31
32
33
34
35
36
37
38
39
40
41
42
43
44
45
46
47
48
49
50
51
52
53
54
55
56
57
58
59
60

2. EXPERIMENTAL

2.1. Fluorophores synthesis

1, 2 and 4 were synthesized according to described procedure¹⁹⁻²¹. To provide 3 in moderate yield, the silver mediated cyclization between 4'-(ethyne-1,2-diyl)bis(N,N-bis(4-methoxyphenyl)aniline) and diphenylphosphine oxide was used (see SI-section 1: Experimental section). The structure of this latter was confirmed by ¹H, ¹³C and ³¹P NMR characterizations (Fig. S1-S3). The thermal behaviour of these four fluorophores was investigated by TGA and DSC analyses (Fig. S4-S11).

2.2. Fabrication of silicone composite films

The two-component silicone polymer (BluesilTM RTV 141 A&B) was composed of a viscous liquid (part A, 90 wt.%), cured by polyaddition reaction with a catalyst (part B, 10 wt.%). Free-standing fluorophore/silicone composite films with 10 wt.% load of fluorophore were obtained as follow. First, the suitable amount of fluorophore was dispersed in part A of silicone with a mechanical mixer (Planetary Centrifugal Vacuum Mixer “Thinky Mixer”) for 10 min at 1200 rpm. The mixture was further homogenized by passing twice through a three-roller mill (Exakt80E). Then, part B of silicone was added to the mixture and homogenized using the mechanical mixer

1
2
3
4 for 10 min at 1200 rpm. Finally, the fluorophore/silicone film (labelled Si-Fx (x =1-4) film (10
5
6
7 wt.%) was casted on a Teflon surface called Elcometer 4340 automatic film applicator at 40°C
8
9
10 (the knife blade height was 200 μ m and the casting speed was 30 mm/s) then cured at 70°C for
11
12
13 another 2 h. The film thickness was measured with an Elcometer 456 coating thickness gauge.
14
15

16 17 **2.3. Characterization techniques** 18

19
20 UV-Visible spectra in solution were recorded at room temperature on a Specord 205
21
22
23 UV/Vis/NIR spectrophotometer. The UV-Vis emission and excitation spectra measurements in
24
25
26 solution were recorded on a FL 920 Edimburgh Instrument equipped with a Hamamatsu R5509-
27
28
29 73 photomultiplier for the NIR domain (300-1700 nm) and corrected for the response of the
30
31
32 photomultiplier. Quantum yield was calculated relative to Rhodamine 6G (Ethanol), $\Phi_{\text{ref}}= 0.94$.
33
34
35
36
37 The photoluminescence quantum yield (PLQY), photoluminescence spectra (PL), and trichromatic
38
39
40 coordinates (CIE x,y) of fluorophores in solid state were recorded with PLQY measurement
41
42
43 software (U6039-05) using an integrating sphere measurement system (C9920-02G) from
44
45
46 Hamamatsu photonics. The setup consisted of a 150 W monochromatic Xe lamp, an integrating
47
48
49 sphere (Spectralon coating, $\varnothing = 3.3$ in.) and a high-sensitivity CCD camera. The internal
50
51
52 photoluminescence quantum yield (PLQY_{int}) and the absorption coefficient (Abs) defined by
53
54
55
56
57
58
59
60

1
2
3
4 formulae (1) and (2) were obtained directly from the measurements made in the integrating sphere.
5

6
7 The absolute photoluminescence quantum yield ($PLQY_{abs}$) was calculated from the product of
8

9
10 $PLQY_{int} \times Abs$, and corresponds to the equation (3).
11

$$12 \quad PLQY_{int} = \frac{\text{number of emitted photons}}{\text{number of absorbed photons}} \quad (1)$$

$$13 \quad Abs = \frac{\text{number of absorbed photons}}{\text{number of incident photons}} \quad (2)$$

$$14 \quad PLQY_{abs} = \frac{\text{number of emitted photons}}{\text{number of incident photons}} \quad (3)$$

15
16
17
18
19
20 Photometric parameters were collected in an integrating sphere with a diode array rapid analyzer
21
22 system (GL Optic integrating sphere GLS 500) at room temperature. Si-Fx films were placed on a
23
24 UV or violet or blue LED emitting respectively at 385 nm, 405 nm, 450 nm and 465 nm. The
25
26
27 testing condition is under a forward current of 800 mA related to an applied voltage of 3.5 V.
28
29
30
31
32

33
34 Reliability studies were carried out on powders (P_1 - P_3) using a home-made set-up consisting of
35
36
37 a power-controlled blue LED emitting at 465 nm as the excitation source and a HR4000 high
38
39
40 resolution spectrometer (Ocean Optics) as the PL analyser. The samples were positioned on a
41
42
43 heating element whose temperature was adjusted to the desired value (room temperature (RT) or
44
45
46
47 100°C). The emission spectra of the fluorophores were acquired every 30 min for 170 hours. Their
48
49
50
51 area was integrated to obtain the total emission intensity. LED power was measured using a
52
53
54
55
56
57
58
59
60 Coherent PowerMax USB PS19Q (19 mm aperture). The measurement was performed by centring

1
2
3 the head unit over the LED source and measuring the power of the LED light emitted through the
4
5
6 aperture. The blue LED power was 183 mW. The LED power density can be expressed in W/m²
7
8
9 and was calculated by LED power (in watt) per unit surface of the sample (0.25 cm²). The power
10
11
12 density of the blue LED was 7300 W/m²; for our experiments, a bandpass filter was used in order
13
14
15
16 to reduce this value to 3080 W/m². The measurements of fluorophores were also carried out with
17
18
19 a UV LED at 375 nm as excitation source to compare their durability to the fourth one (**P₄**) which
20
21
22 cannot be excited suitably by the blue LED. The complete system (UV LED + collimating lenses
23
24
25
26 + filters) irradiates the sample under a photon flux of 900 W/m².
27
28
29
30
31
32

33 34 **3. RESULTS AND DISCUSSIONS**

35 36 37 **3.1. Optical characterization of fluorophores in solution in dichloromethane at 298K**

38
39
40 The spectroscopic properties of the four fluorophores 1-4 (**Table 2**) were investigated in diluted
41
42
43 dichloromethane (DCM) solutions ($c \approx 1.10^{-6}$ mol.L⁻¹). As described by Songpan Xu et al ²², 1-2
44
45
46 display similar absorption properties with an intense band between 350 nm and 425 nm ($\lambda_{\max}(2) =$
47
48
49 398 nm; $\lambda_{\max}(1) = 403$ nm) (**Fig. 1a**) attributed to π - π^* transition. Diphenylbenzophosphole
50
51
52 oxide (sample 4) exhibits a band at 346 nm, which is attributed to π - π^* transition centered on the
53
54
55
56
57
58
59
60

1
2
3 benzophosphole core ²³. Fluorophore **3** displays a different absorption spectrum compared to **4**,
4
5
6
7 with a band centered at 300 nm which is attributed to π - π^* transition centered on the
8
9
10 benzophosphole core and another much wider and less intense band in the visible range
11
12
13 ($\lambda_{\text{max}}(\mathbf{3}) = 422 \text{ nm}$) attributed to Internal Charge Transfer (ICT) from the arylamine donor to the
14
15
16 benzophosphole oxide acceptor as it has been reported for similar compound ^{9, 24}. As can be seen
17
18
19 in **Table 2**, chromophores **1** and **2** show intense fluorescence with maximum emission wavelengths
20
21
22 at 431 nm and 430 nm respectively (**Fig. 1b**), with high PLQY_{int} , close to 100%. **4** displays
23
24
25 fluorescence with a maximum wavelength at 462 nm with a low PLQY_{int} of less than 1%, in
26
27
28 adequation with its “aggregation induced emission” character ²³. Due to the presence of electron-
29
30
31 rich ICT-inducing moieties, **3** displays a red-shifted fluorescence with a maximum wavelength at
32
33
34 632 nm with a PLQY_{int} of 17% ²⁵. Furthermore, we can point out that the emission profile of **3-4**
35
36
37
38
39
40
41 is rather broad compared to **1-2**.
42
43
44
45
46
47
48
49
50
51
52
53
54
55
56
57
58
59
60

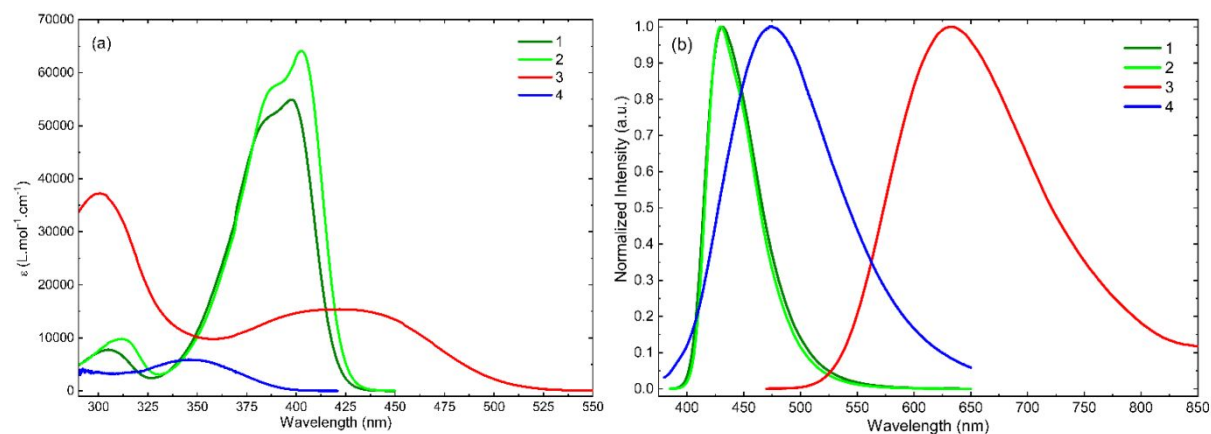


Fig. 1. (a) UV-vis absorption and (b) emission spectra of 1-4 in diluted DCM solution

($\lambda_{\text{exc}} = \lambda_{\text{abs max}}$ reported in the **Table 1** for each fluorophore)

The excitation spectra of fluorophores 1-4 in diluted DCM solution are presented in **Fig. S12**.

Table 2. Spectroscopic data of 1-4 in diluted DCM ($c \approx 1.10^{-6}$ mol.L⁻¹)

Fluorophores	$\lambda_{\text{abs max}}$ (nm)	ϵ (L.mol ⁻¹ .cm ⁻¹) ^a	$\lambda_{\text{em max}}$ (nm)	PLQY _{abs} ^e (%)
1^b	403	64000	430	99
2^c	398	55000	431	99
3	422	15000	632	23
4^d	346	5900	462	<1%

^a ϵ : molar absorption coefficient, ^b data from reference²⁰, ^c data from reference²², ^d data from reference²³, ^e Absolute Quantum yield measured on the same integration sphere

3.2. Optical characterization of fluorophores in solid state

1
2
3
4 In order to assess the ability of fluorophores **1-4** to be used as DC phosphors in LED devices,
5
6
7 their absolute photoluminescent quantum yields ($PLQY_{abs}$) were recorded in solid state (powder
8
9
10 sample) from 250 nm to 550 nm (**Fig. 2**). All of them exhibit high $PLQY_{abs}$ between 30% and 70%
11
12
13 in the UV/blue excitation range, except **P₄** whose $PLQY_{abs}$ drops drastically after 420 nm, in
14
15
16 agreement with its UV-vis absorption spectrum. Thus, regarding their $PLQY_{abs}$ values (**Table 3**),
17
18
19 fluorophores **P_x** (x =1-3) can be combined efficiently with commercial UVA/violet/blue LED chips
20
21
22
23 whereas **P₄** can only be excited by UVA/violet LED chips (365 nm, 385 nm or 405 nm). As
24
25
26
27 expected, based on the literature reports, all those fluorophores display good luminescent quantum
28
29
30 yields in the solid-state.
31
32
33
34
35
36
37
38
39
40
41
42
43
44
45
46
47
48
49
50
51
52
53
54
55
56
57
58
59
60

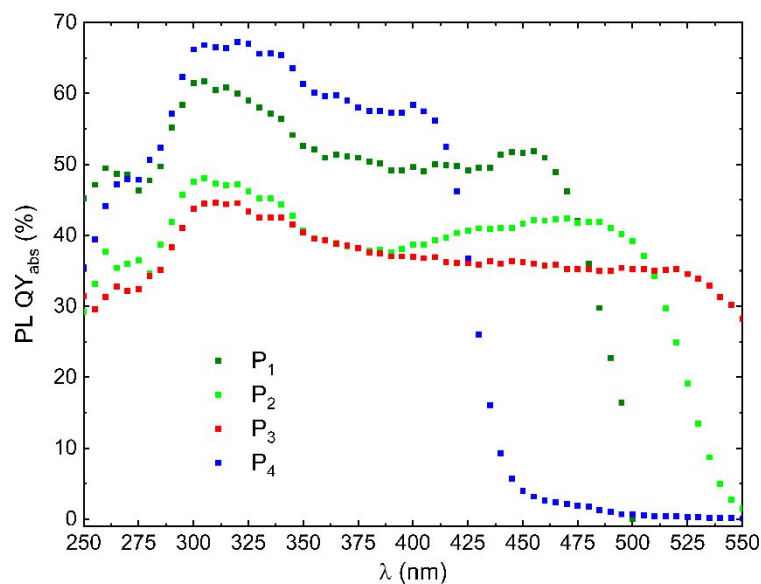


Fig. 2. $PLQY_{abs}$ of solid-state fluorophores P_x ($x = 1-4$) recorded upon excitation from 250 to 550

nm

Table 3. $PLQY_{abs}$ (%) of P_x ($x = 1-4$) upon excitation at wavelengths of commercial LED chips

λ_{exc}	UVA LED		Violet LED	Blue LED	
	365 nm	385 nm	405 nm	450 nm	465 nm
P1	51	50	49	52	49
P2	39	38	39	42	42
P3	39	38	37	36	36
P4	60	58	58		

1
2
3 Emission spectra were recorded at RT upon excitation at 405 nm for \mathbf{P}_x ($x=1-4$) samples (**Fig.**
4
5
6
7 **3**). All those compounds display strong luminescence in powder with a gradual red-shift in the
8
9
10 series \mathbf{P}_4 - \mathbf{P}_1 - \mathbf{P}_2 - \mathbf{P}_3 ($\lambda_{\text{em max}}(1) = 460$ nm; $\lambda_{\text{em max}}(2) = 500$ nm; $\lambda_{\text{em max}}(3) = 560$ nm; $\lambda_{\text{em max}}(4) =$
11
12
13 616 nm). The solid-state luminescence of the boron difluoride complexes **1-2** markedly differ from
14
15
16 the diluted solution, due to intermolecular interactions in the condense phase. This aspect has been
17
18
19 previously investigated experimentally and theoretically ^{12, 20, 26}. On the contrary, for
20
21
22 benzophospholes **3-4**, there is no significant modification between the solution and the solid-state,
23
24
25 as usually observed ^{8, 9, 23}. We should also point out that the emission spectra of the \mathbf{P}_x ($x=1-4$)
26
27
28 fluorophores do not change with the change in excitation wavelength, as shown in **Fig. S13**. The
29
30
31 excitation spectra of fluorophores \mathbf{P}_1 - \mathbf{P}_4 are displayed in **Fig. S14**.
32
33
34
35
36
37
38
39
40
41
42
43
44
45
46
47
48
49
50
51
52
53
54
55
56
57
58
59
60

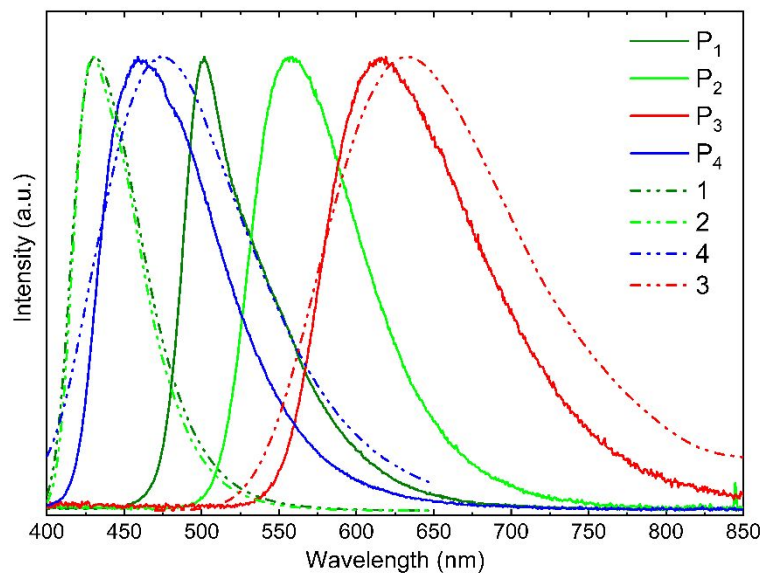


Fig. 3. Emission spectra recorded at RT from solid state fluorophores in solid curve (P_1 – P_4) and in diluted DCM solution in dashed curve (1-4) upon excitation at 405 nm

We thus have in hand a series of fluorophores emitting respectively in the Blue, Green, Yellow and Red wavelength range as powders. The associated CIE chromatic coordinates (**Fig. 4**) highlight the bathochromic emission shift occurring when switching from powders P_4 to P_1 , P_2 and P_3 . As a result, by mixing these fluorophores in solid state (P_x ($x=1-4$)) in the right proportion, we should be able to produce white light with controlled photometric parameters.

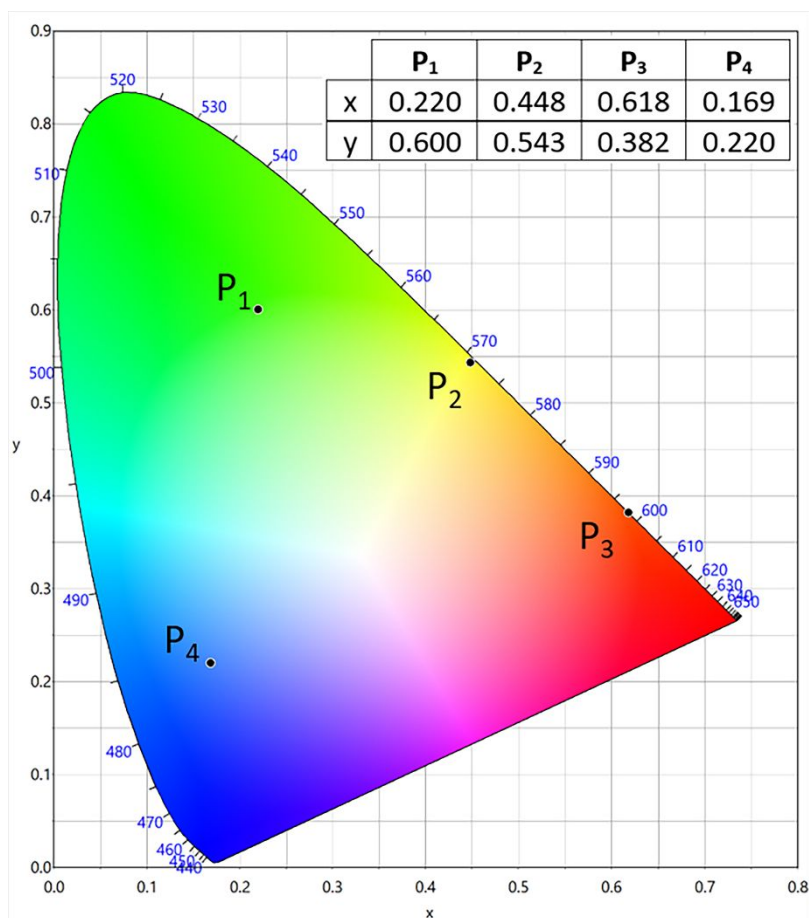


Fig. 4. Chromaticity coordinates of P_x ($x=1-4$) fluorophores in solid state with the CIE chromaticity coordinates excited by a 465nm blue light for P_1 , P_2 and P_3 , and excited by a 405 nm UV light for P_4 .

Interestingly, the emission spectrum of compound P_2 recorded upon excitation at 465 nm (**Fig. 5**) overlaps very well with the emission spectrum of YAG:Ce (Ce^{3+} doped $Y_3Al_5O_{12}$) which is the reference yellow phosphor used in all white light emitting diodes (WLEDs).

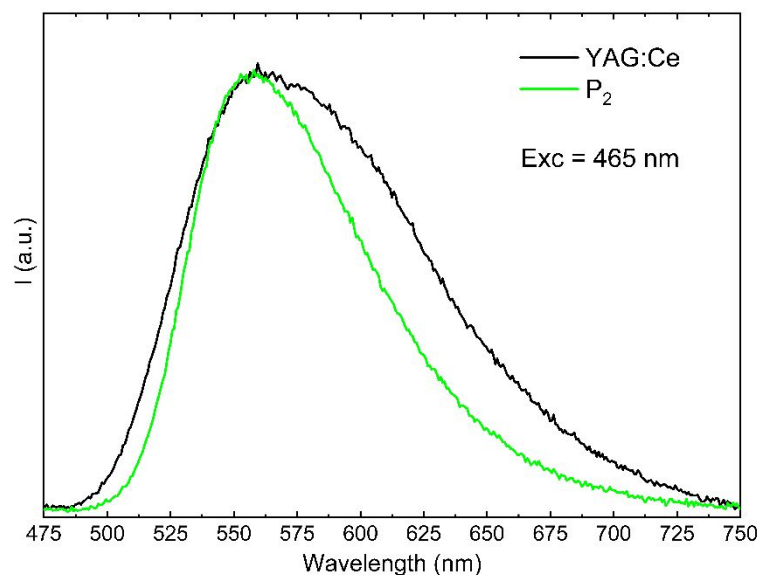


Fig. 5. Comparison of normalized emission spectra of **P₂** and commercial YAG:Ce upon excitation at 465 nm

3.3. Optical characterization of luminescent composite films

3.3.1. Emission spectra and colorimetry

To further investigate the suitability of the selected fluorophore powders for LED applications, composite films were prepared by dispersing the powder in a silicone elastomer (PDMS-type) matrix (according to the protocol described in the experimental part) (**Fig. 6**). Four composite films, named **Si-F_x** ($x = 1, 2, 3$ or 4) (**Si-F₁** for example refers to the films elaborated with 10wt.% of fluorophore **P₁**) were prepared. For each film, the measured thickness is of the order of $110 \pm 5 \mu\text{m}$.

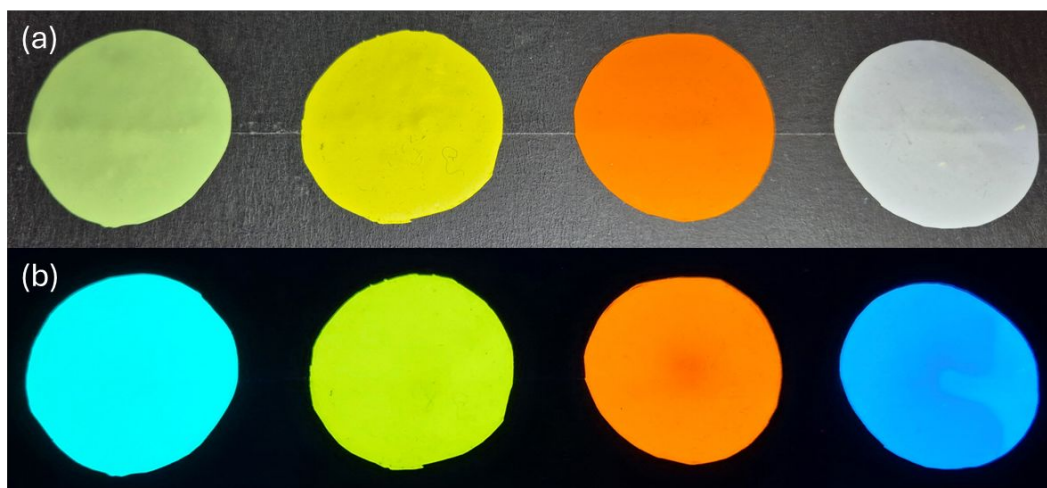


Fig. 6. Pictures of compounds Si-F_x ($x=1-4$) composite films under (a) daylight and (b) UV light 365nm

The emission spectra of the Si-F_x ($x=1-3$) and Si-F_4 composite films were recorded under excitation at 465 nm and 405 nm respectively (**Fig. 7a** solid lines) and were compared with those of powders (**Fig. 7a** dotted lines).

Analysis of **Fig. 7a** reveals a shift in the emission maximum towards shorter wavelengths for the four composite films compared with their powder counterparts. This behaviour has already been observed for composite films produced using the same procedure as that described in this paper²⁷ and can be explained by a disaggregation effect of the powders induced by the rolling step during film preparation. We can also point out that the differences between the emission spectra are more marked for blue and green powders and films. This suggests that fluorophores **4** and **1** are more

1
2
3
4 sensitive to roll milling-induced shear forces than fluorophores **2** and **3**. As a result, the
5
6
7 chromaticity diagram shows slightly different color points for red and yellow powders and films.
8
9

10 These differences are more pronounced for green and blue powders and films (**Fig. 7b**).
11
12
13
14
15
16
17
18
19
20
21
22
23
24
25
26
27
28
29
30
31
32
33
34
35
36
37
38
39
40
41
42
43
44
45
46
47
48
49
50
51
52
53
54
55
56
57
58
59
60

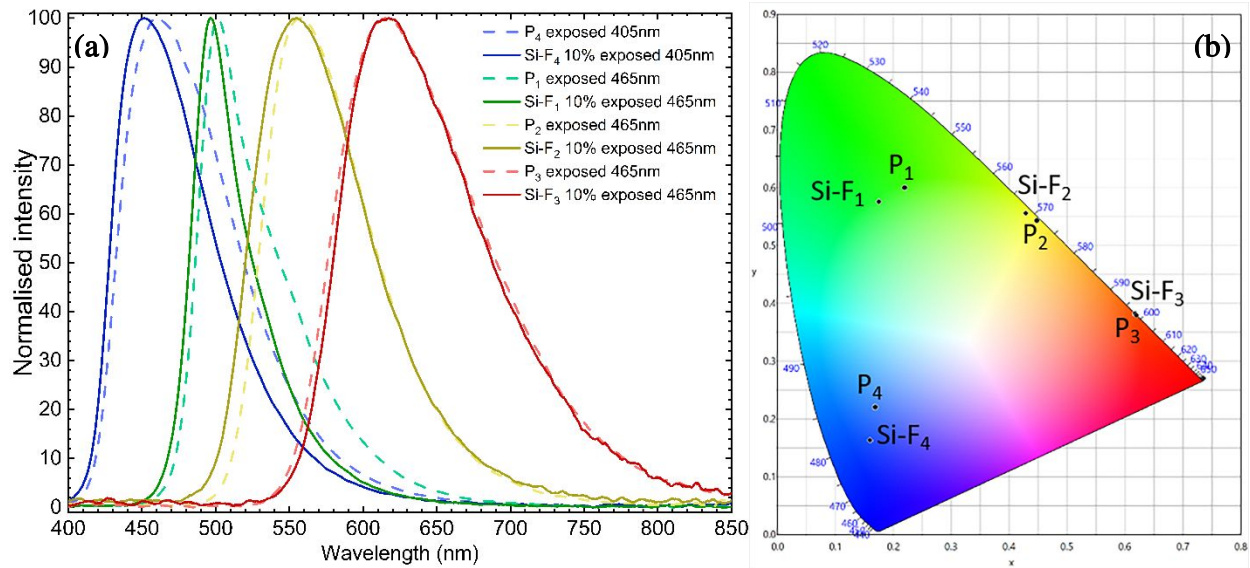


Fig. 7. a) Emission spectra of the **Si-F_x** ($x=1-4$); b) CIE chromaticity coordinates of powders and **Si-F_x** composite film upon 465 nm for powders **P₁**, **P₂** and **P₃** and the corresponding films and 405 nm for powder **P₄** and **Si-F₄**.

3.3.2. PLQY_{abs} of Si-F_x composite film

PLQY_{abs} of the **Si-F_x** ($x=1-4$) composite films were recorded for excitation wavelengths from 250 to 550 nm (**Fig. 8**). The films exhibit PLQY_{abs} comparable to those of powders, meaning that the dispersion in silicone did not modify photoluminescence behaviour. A more detailed analysis of the evolution of the PLQY_{abs} even shows a slight increase in the performance of the films compared to the powders. This can be explained by the dispersion effect generated by the polymer

1
2
3
4 matrix, which leads to a reduction in non-radiative energy transfer and, consequently, to an
5
6
7 improved internal quantum yield, as illustrated in **Figs. S15** and **S16**.
8
9
10
11
12
13
14
15
16
17
18
19
20
21
22
23
24
25
26
27
28
29
30
31
32
33
34
35
36
37
38
39
40
41
42
43
44
45
46
47
48
49
50
51
52
53
54
55
56
57
58
59
60

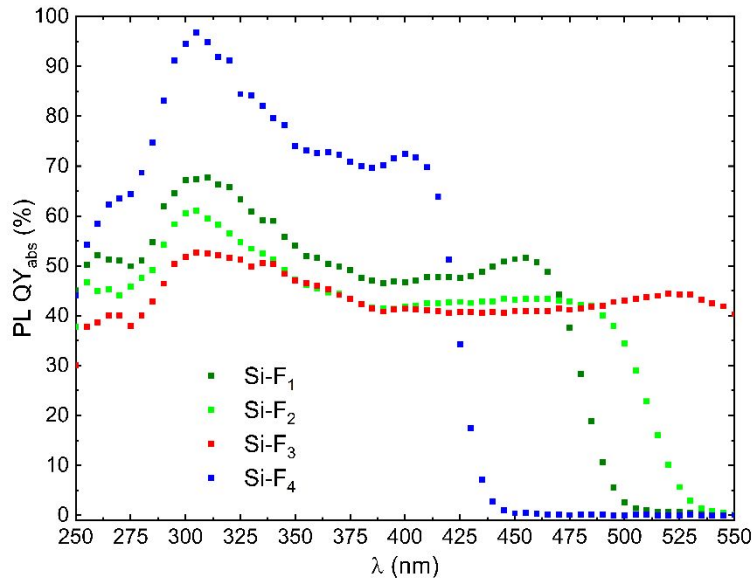


Fig. 8. $PLQY_{abs}$ of composite films $Si-F_x$ ($x = 1-4$) recorded upon excitation from 250 to 550 nm.

3.3.3. White light emission produced by the association of a blue or a UV LED chip and several $Si-F_x$ ($x=1-4$) films

As these composites emit in the blue, green, yellow, or red parts of the spectrum, they can be combined to generate white light under blue or UV excitation. Consequently, several suitable combinations of these films with commercial blue or UV LEDs were tested. The three devices that yielded the highest Color Rendering Index (CRI) are presented (**Fig. 9**). Many other combinations were explored by varying the concentration of phosphors in the composite coating and also by adjusting the thickness of these coatings. The photometric parameters related to these different prototypes are summarized in **Table S1**.

- 1
2
3
4 ➤ Blue LED emitted at 465 nm + **Si-F₃** (5%wt / 100 μm) + **Si-F₂** (5%wt / 200 μm) + **Si-F₁**
5
6
7 (5%wt / 100 μm) (**Fig. 9a**).8
9
10 ➤ Blue LED emitted at 450 nm + **Si-F₃** (5%wt / 100 μm) + **Si-F₂** (5%wt / 100 μm) + **Si-F₁**
11
12
13 (5%wt / 100 μm) (**Fig. 9b**).14
15
16
17 ➤ Violet LED emitted at 405 nm **Si-F₃** (5%wt / 100 μm) + **Si-F₂** (2%wt / 100 μm) + **Si-F₁**
18
19
20 (2%wt / 100 μm) + **Si-F₄** (10%wt / 200 μm) (**Fig. 9c**).21
22

23
24 The three configurations studied lead to characteristic emission spectra. This is explained in
25
26 particular by the greater or lesser absorption of the emission from the LED used and by the
27
28 reabsorption phenomena that will take place given the overlap of the emission spectra.
29
30
31

32
33 As shown in **Fig. 9d**, these specific characteristics allow the photometric parameters to be
34
35 modulated including white light emission.
36
37
38

39
40 This study thus show that a combination of the fluorophores described in this article can be
41
42 successfully used as REEs free DC phosphors.
43
44
45
46
47
48
49
50
51
52
53
54
55
56
57
58
59
60

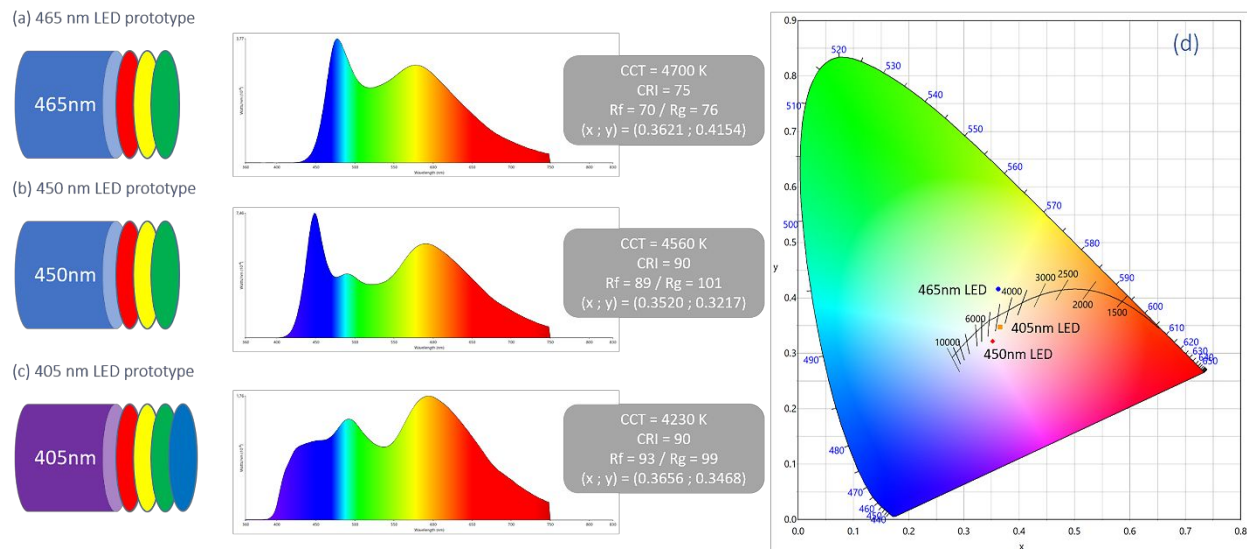


Fig. 9. Spectrometric and photometric properties of white LED prototypes designed using a combination of different commercial LEDs (465 nm (a), 450 nm (b) and 405 nm (c)) with a superposition of composite films: one red, one yellow, one green and one blue for the 405 nm LED and (d) CIE chromaticity coordinates of the three combinations (LED/Si-F_x Films)

3.4. Stability study of fluorophores upon thermal and photonic stresses

Stability under photonic and thermal stresses is an important parameter for LED applications.

To study aging phenomena, samples P_x ($x=1-4$) were exposed for several hours to the radiation from a commercial UV LED emitting at 375 nm. The behavior of powders P_x ($x=1-3$) was also studied under irradiation with a commercial blue LED emitting at 465 nm.

Under excitation at 465 nm with a flux of 3080 W/m², it is observed that the fluorophore P_3 (based on an organophosphorus emitter) degrades much more rapidly than the boron difluoride complexes (P_1 and P_2) (**Fig. 10a**). Indeed, after 20 hours of irradiation, P_3 is almost extinguished, whereas P_1 and P_2 retain approximately 60% and 70% of their initial emission intensity, respectively, and their performance remains nearly constant over the studied exposure time.

The same study conducted under excitation with a UV LED emitting at 375 nm. (a wavelength suitable for studying P_4), highlights that P_2 remains the most stable fluorophore (**Fig. 10b**). It retains more than 80% of its emission after 7 days of aging. P_1 and P_4 , on the other hand, retain nearly 50% of their initial emission over the same period. The red fluorophore P_3 experiences a significant decrease in its emission intensity, similar to that observed under blue excitation, and is nearly extinguished after only 40 hours of irradiation. The emission spectra recorded during the

1
2
3 aging process for these powders are shown in **Fig. S17**. They exhibit the same spectral profile
4
5
6
7 throughout aging, with only a decrease in intensity. This leads us to conclude that the studied
8
9
10 molecules are being destroyed rather than modified under the influence of the photon flux.

11
12
13 As expected, the combined action of photon and thermal stress accelerates the degradation for
14
15
16 all studied samples. For instance, the **P₁** powder, which was the most stable at 20°C, showing only
17
18
19 a 20% decrease in emission after 160 hours of irradiation, experiences a 60% intensity drop when
20
21
22
23 a temperature of 100°C is applied (**Fig. S18**).

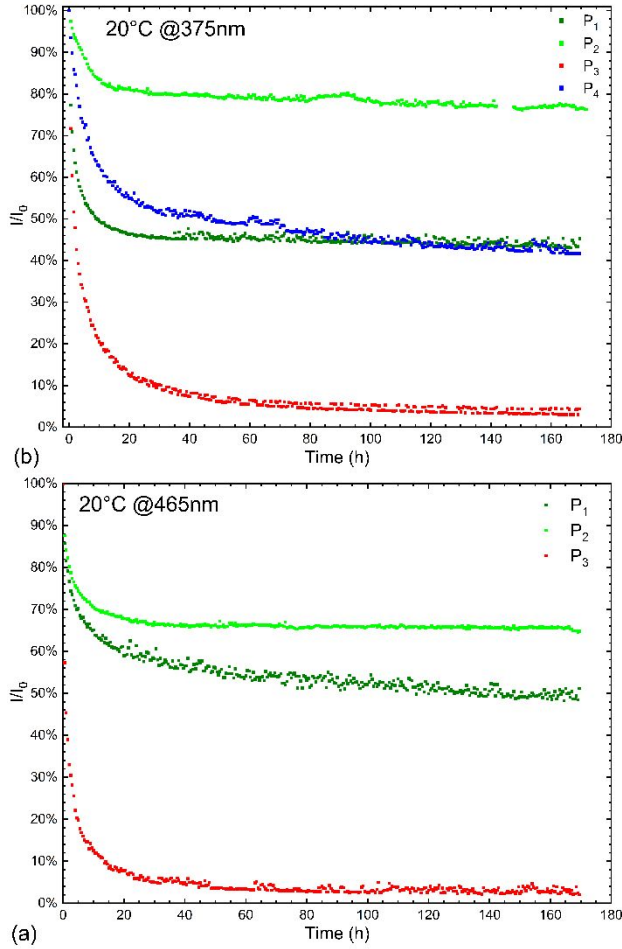


Fig. 10. Evolution of the emission (integrated intensity) as a function of irradiation time under (a) blue LED (465nm) and (b) under UV LED (375 nm) at 20°C

We deliberately worked under stringent conditions to highlight the stresses to avoid in order to preserve satisfactory emission properties. From this study, it is important to note that matrices P_1 , P_2 , and P_4 exhibit promising performance under blue and UV LED excitation, even under photon

1
2
3 stress. This suggests their potential use in various applications such as displays, anti-counterfeiting
4
5
6
7 marking, and more.
8
9

10 4. CONCLUSIONS

11
12
13 This work explores the potential of rare-earth-free phosphors for white light-emitting diodes
14 (WLEDs) as a sustainable and cost-effective alternative to conventional phosphors containing rare-
15
16 earth elements. We focused our attention on organic fluorophores, particularly π -extended
17 phospholes and difluoroboron β -diketonates. The different fluorophores (**P₁-P₄**) were
18
19 characterized by a high photoluminescence absolute quantum yield and a wide range of emission
20 colors (B, G, Y and R). The fabrication of silicone/fluorophores composite films, **Si-F_x** (x=1-4)
21
22 exhibiting similar properties than phosphors powders, further validated their potential for LED
23
24 applications. Various WLEDs prototypes with tunable color correlated temperature are presented,
25
26 demonstrating the feasibility of producing white light emission through the careful combination of
27
28 red, yellow, green, and blue-emitting films. Furthermore, the stability of their optical properties
29
30 under thermal and photonic stresses highlighted the robustness of the fluorophores **P₁**, **P₂** and **P₄**,
31
32 especially under UV and blue LED excitation. In summary, the development of these rare-earth-
33
34
35
36
37
38
39
40
41
42
43
44
45
46
47
48
49
50
51
52
53
54
55
56
57
58
59
60

1
2
3 free organic fluorophores presents a compelling avenue for advancing the field of LED technology,
4
5
6 offering sustainable alternatives with tunable properties and enhanced stability.
7
8
9

10 5. SUPPORTING INFORMATION

11
12
13 Synthesis description and NMR spectra (^1H , ^{13}C , ^{31}P) of compound 3; TGA and DSC curves of
14
15
16 all compounds; additional experimental details about emission spectra; PLQY_{int} of powders and
17
18
19 films; degradation evolution and all LED configurations tested.
20
21
22

23 6. AUTHOR CONTRIBUTIONS

24
25
26
27 The manuscript was written through contributions of all authors.
28
29

30 7. CONFLICTS OF INTEREST

31
32
33 There are no conflicts of interest to declare.
34
35
36

37 8. REFERENCES

- 38
39
40 1. Piquette, A.; Bergbauer, W.; Galler, B.; Mishra, K. C., On Choosing Phosphors for Near-
41 UV and Blue LEDs for White Light. *ECS Journal of Solid State Science and Technology* **2016**, *5*
42 (1), R3146.
43
44 2. Gao, T.; Tian, J.; Liu, Y.; Liu, R.; Zhuang, W., Garnet phosphors for white-light-emitting
45 diodes: modification and calculation. *Dalton Transactions* **2021**, *50*(11), 3769-3781.
46
47 3. Li, J.; Yan, J.; Wen, D.; Khan, W. U.; Shi, J.; Wu, M.; Su, Q.; Tanner, P. A., Advanced
48 red phosphors for white light-emitting diodes. *Journal of Materials Chemistry C* **2016**, *4* (37),
49 8611-8623.
50
51
52
53
54
55
56
57
58
59
60

- 1
2
3
4 4. Binnemans, K.; Jones, P. T.; Blanpain, B.; Van Gerven, T.; Yang, Y.; Walton, A.;
5 Buchert, M., Recycling of rare earths: a critical review. *Journal of Cleaner Production* **2013**, *51*,
6 1-22.
- 7
8 5. Tkaczyk, A. H.; Bartl, A.; Amato, A.; Lapkovskis, V.; Petranikova, M., Sustainability
9 evaluation of essential critical raw materials: cobalt, niobium, tungsten and rare earth elements.
10 *Journal of Physics D: Applied Physics* **2018**, *51* (20), 203001.
- 11
12 6. Lukowiak, A.; Zur, L.; Tomala, R.; LamTran, T. N.; Bouajaj, A.; Streck, W.; Righini,
13 G. C.; Wickleder, M.; Ferrari, M., Rare earth elements and urban mines: Critical strategies for
14 sustainable development. *Ceramics International* **2020**, *46* (16, Part B), 26247-26250.
- 15
16 7. Ricci, P. C., Assessment of Crystalline Materials for Solid State Lighting Applications:
17 Beyond the Rare Earth Elements. *Crystals* **2020**, *10* (7), 559.
- 18
19 8. Duffy, M. P.; Delaunay, W.; Bouit, P. A.; Hissler, M., π -Conjugated phospholes and their
20 incorporation into devices: components with a great deal of potential. *Chemical Society Reviews*
21 **2016**, *45* (19), 5296-5310.
- 22
23 9. Zhuang, Z.; Bu, F.; Luo, W.; Peng, H.; Chen, S.; Hu, R.; Qin, A.; Zhao, Z.; Tang, B.
24 Z., Steric, conjugation and electronic impacts on the photoluminescence and electroluminescence
25 properties of luminogens based on phosphindole oxide. *Journal of Materials Chemistry C* **2017**, *5*
26 (7), 1836-1842.
- 27
28 10. Kim, D.-H.; D'Aléo, A.; Chen, X.-K.; Sandanayaka, A. D. S.; Yao, D.; Zhao, L.;
29 Komino, T.; Zaborova, E.; Canard, G.; Tsuchiya, Y.; Choi, E.; Wu, J. W.; Fages, F.; Brédas,
30 J.-L.; Ribierre, J.-C.; Adachi, C., High-efficiency electroluminescence and amplified spontaneous
31 emission from a thermally activated delayed fluorescent near-infrared emitter. *Nature Photonics*
32 **2018**, *12* (2), 98-104.
- 33
34 11. Archet, F.; Yao, D.; Chambon, S.; Abbas, M.; D'Aléo, A.; Canard, G.; Ponce-Vargas,
35 M.; Zaborova, E.; Le Guennic, B.; Wantz, G.; Fages, F., Synthesis of Bioinspired Curcuminoid
36 Small Molecules for Solution-Processed Organic Solar Cells with High Open-Circuit Voltage.
37 *ACS Energy Letters* **2017**, *2* (6), 1303-1307.
- 38
39 12. D'Aléo, A.; Sazzad, M. H.; Kim, D. H.; Choi, E. Y.; Wu, J. W.; Canard, G.; Fages, F.;
40 Ribierre, J. C.; Adachi, C., Boron difluoride hemicurcuminoid as an efficient far red to near-
41 infrared emitter: toward OLEDs and laser dyes. *Chemical Communications* **2017**, *53* (52), 7003-
42 7006.
- 43
44
45
46
47
48
49
50
51
52
53
54
55
56
57
58
59
60

13. Li, P.; Liang, Q.; Hong, E. Y.-H.; Chan, C.-Y.; Cheng, Y.-H.; Leung, M.-Y.; Chan, M.-Y.; Low, K.-H.; Wu, H.; Yam, V. W.-W., Boron(iii) β -diketonate-based small molecules for functional non-fullerene polymer solar cells and organic resistive memory devices. *Chemical Science* **2020**, *11* (42), 11601-11612.
14. Fave, C.; Cho, T.-Y.; Hissler, M.; Chen, C.-W.; Luh, T.-Y.; Wu, C.-C.; Réau, R., First Examples of Organophosphorus-Containing Materials for Light-Emitting Diodes. *Journal of the American Chemical Society* **2003**, *125* (31), 9254-9255.
15. Fadhel, O.; Gras, M.; Lemaitre, N.; Deborde, V.; Hissler, M.; Geffroy, B.; Réau, R., Tunable Organophosphorus Dopants for Bright White Organic Light-Emitting Diodes with Simple Structures. *Advanced Materials* **2009**, *21* (12), 1261-1265.
16. Wang, C.; Fukazawa, A.; Taki, M.; Sato, Y.; Higashiyama, T.; Yamaguchi, S., A Phosphole Oxide Based Fluorescent Dye with Exceptional Resistance to Photobleaching: A Practical Tool for Continuous Imaging in STED Microscopy. *Angewandte Chemie International Edition* **2015**, *54* (50), 15213-15217.
17. Gaffen, J. R.; Bentley, J. N.; Torres, L. C.; Chu, C.; Baumgartner, T.; Caputo, C. B., A Simple and Effective Method of Determining Lewis Acidity by Using Fluorescence. *Chem* **2019**, *5* (6), 1567-1583.
18. Wang, C.; Taki, M.; Sato, Y.; Fukazawa, A.; Higashiyama, T.; Yamaguchi, S., Super-Photostable Phosphole-Based Dye for Multiple-Acquisition Stimulated Emission Depletion Imaging. *Journal of the American Chemical Society* **2017**, *139* (30), 10374-10381.
19. Cogné-Laage, E.; Allemand, J.-F.; Ruel, O.; Baudin, J.-B.; Croquette, V.; Blanchard-Desce, M.; Jullien, L., Diaroyl(methanato)boron Difluoride Compounds as Medium-Sensitive Two-Photon Fluorescent Probes. *Chemistry – A European Journal* **2004**, *10* (6), 1445-1455.
20. Zhang, G.; Lu, J.; Sabat, M.; Fraser, C. L., Polymorphism and Reversible Mechanochromic Luminescence for Solid-State Difluoroboron Avobenzone. *Journal of the American Chemical Society* **2010**, *132* (7), 2160-2162.
21. Unoh, Y.; Hirano, K.; Satoh, T.; Miura, M., An Approach to Benzophosphole Oxides through Silver- or Manganese-Mediated Dehydrogenative Annulation Involving C \square C and C \square P Bond Formation. *Angewandte Chemie International Edition* **2013**, *52* (49), 12975-12979.
22. Xu, S.; Evans, R. E.; Liu, T.; Zhang, G.; Demas, J. N.; Trindle, C. O.; Fraser, C. L., Aromatic Difluoroboron β -Diketonate Complexes: Effects of π -Conjugation and Media on Optical Properties. *Inorganic Chemistry* **2013**, *52* (7), 3597-3610.

- 1
2
3
4 23. Bu, F.; Wang, E.; Peng, Q.; Hu, R.; Qin, A.; Zhao, Z.; Tang, B. Z., Structural and
5 Theoretical Insights into the AIE Attributes of Phosphindole Oxide: The Balance Between Rigidity
6 and Flexibility. *Chemistry – A European Journal* **2015**, *21* (11), 4440-4449.
7
8 24. Ledos, N.; Tondelier, D.; Geffroy, B.; Jacquemin, D.; Bouit, P.-A.; Hissler, M., Reaching
9 the 5% theoretical limit of fluorescent OLEDs with push–pull benzophospholes. *Journal of*
10 *Materials Chemistry C* **2023**, *11* (11), 3826-3831.
11
12 25. Kuno, J.; Ledos, N.; Bouit, P.-A.; Kawai, T.; Hissler, M.; Nakashima, T., Chirality
13 Induction at the Helically Twisted Surface of Nanoparticles Generating Circularly Polarized
14 Luminescence. *Chemistry of Materials* **2022**, *34* (20), 9111-9118.
15
16 26. Wilbraham, L.; Louis, M.; Alberga, D.; Brosseau, A.; Guillot, R.; Ito, F.; Labat, F.;
17 Métivier, R.; Allain, C.; Ciofini, I., Revealing the Origins of Mechanically Induced Fluorescence
18 Changes in Organic Molecular Crystals. **2018**, *30* (28), 1800817.
19
20 27. Legentil, P.; Leroux, F.; Therias, S.; Boyer, D.; Chadeyron, G., Sulforhodamine B-LDH
21 composite as a rare-earth-free red-emitting phosphor for LED lighting. *Journal of Materials*
22 *Chemistry C* **2020**, *8* (34), 11906-11915.
23
24
25
26
27
28
29
30
31
32
33
34
35
36
37
38
39
40
41
42
43
44
45
46
47
48
49
50
51
52
53
54
55
56
57
58
59
60

Combining organic fluorophores for high performances WLEDs

